Inelastic collisions in the $He^+ + H_2$ system at low-keV energies*

A. V. Bray,†‡ D. S. Newman, and E. Pollack
Department of Physics, University of Connecticut, Storrs, Connecticut 06268
(Received 6 December 1976)

The direct and charge-exchange scattering is studied in the $He^+ + H_2$ collision system. Charge exchange, which is investigated at energies from 0.5 to 3.0 keV and at angles out to 12°, rapidly becomes the most important collision process as the scattering angle increases. At least two dominant channels contribute to the charge exchange. Direct scattering is studied at 1.0, 2.0, and 3.0 keV and at small angles. The direct scattering shows He^+ energy-loss spectra having four peaks representing elastic scattering and inelastic processes resulting from vibro-rotational excitation of the ground and electronically excited states of H_2 and H_2^+. It is shown that the collision involves the entire molecule and that there is negligible coupling between the electronic and vibro-rotational excitation. Reduced cross-section plots for the observed direct scattering exhibit a behavior suggesting that the inelastic processes result from interactions occurring at particular interparticle separations.

I. INTRODUCTION

Atomic collisions have been studied both theoretically and experimentally for many years. Although it was recognized that inelastic collisions would occur (even at energies just above threshold), detailed studies only recently became possible with the development of refined experimental and theoretical approaches. In particular rapid progress in our understanding of atomic collisions followed the introduction of collision spectroscopy techniques to scattering experiments. In these experiments the angular and energy distributions of scattered particles are determined and provide information on the participating states as well as on important collision parameters such as the distance of closest approach. The detailed information obtained stimulated the development of the necessary theory and greatly increased our understanding of the dynamics of atomic collisions. The application of collision spectroscopy to ion-molecule systems is a more recent development, and there are few papers to cite which make the required measurements. The present work shows that collision spectroscopy can indeed provide significant information, even on these more complex collisions.

Although ion-molecule collisions occur frequently and are important in determining the behavior of a large number of systems including gaseous discharges and the atmosphere, little theoretical work has been done on such collisions. This is of course understandable since the problems involved are formidable. Contributing to the difficulties is the availability of many inelastic channels, even at very low energies. The molecules can be electronically and vibro-rotationally excited, they can dissociate, charge-exchange processes can occur, and the atomic projectiles are subject to excitation.

In the ion-atom and atom-atom cases the experimental results led to the development of useful models and suggested theoretical approximations which could be applied to the problems. The theory was rather rapidly advanced to the point where good agreement between theory and experiment could be achieved in many cases. In the ion-molecule problem there are several possible simplifications that can be made in the theoretical treatment. In the case of homonuclear molecules the g or u symmetry of the molecular states may play an important role in limiting the possible outgoing channels. The relative importance of Σ-Σ, Σ-Π, etc. transitions in the molecule can allow for further simplification. In addition the recent work of Fernandez,[1c] on $Ar^+ + N_2$, demonstrated that the electronic and vibro-rotational excitation of the N_2 resulting from the collision occurs independently, thus allowing a separation of the problem into two simpler ones.

The present work[2,3] on $He^+ + H_2$ is basically similar to that done on $Ar^+ + N_2$. The current studies are more detailed however and include determinations of cross sections.

II. EXPERIMENTAL METHODS AND RESULTS

The apparatus and most of the experimental techniques employed have been previously described[1,4] and are only outlined here. Figure 1 shows the experimental arrangement. He^+ ions produced by electron bombardment in an ion source are extracted, mass-analyzed, and focused into a beam by an ion optics system employing cylindrical electrostatic lenses. The resulting He^+ beam is collimated and enters a scattering

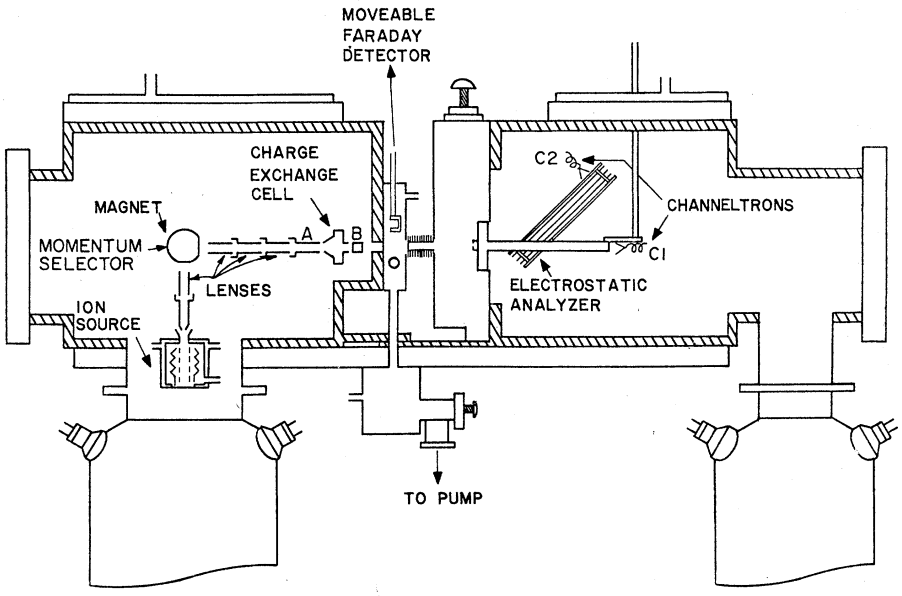

FIG. 1. Schematic of the apparatus.

cell containing H_2 at low pressure. A fraction of the beam, scattered through an angle θ, enters a detector chamber positioned at θ. The scattered beam then passes through the entrance slit on the front plate of a 13-cm-long parallel-plate electrostatic energy analyzer which scans the energy spectrum of the scattered He^+. Scattered He^0 (from charge-exchange collisions) passes through the analyzer and exits from a slit on the rear plate. During operation the front analyzer plate is grounded while the voltage on the rear plate is varied. Channeltron electron multipliers located behind each exit slit of the analyzer detect the energy-analyzed ion and the undeflected neutral components of the scattered beam. For studies of direct scattering, the entrance and exit slits are typically set at effective widths of 0.0038 and 0.0025 cm, respectively. The measured full width at half maximum (FWHM) of the incident beam is about 0.6 eV at 1 keV. Energy-loss spectra (ELS) are obtained by a multiscaling technique which has been described in detail elsewhere.[5] For measurements of the probability of electron capture the analyzer slits are kept fully opened (0.6 cm). The beams have a calculated FWHM angular profile of $0.17°$ for $0 < \theta < 1.25°$ and $0.28°$ for $1.0° < \theta < 2.5°$ for the ELS measurements. In measurements of the probability of electron capture the FWHM is $0.28°$ for $0 < \theta < 2.5°$ and $0.68°$ for $2° < \theta$. The measured FWHM is usually narrower than the calculated values stated.[1]

A. Determination of the total differential cross sections

The "total" (independent of charge state and energy loss) differential cross section $\sigma(\theta)$ may be obtained from[6]

$$\sigma(\theta) = \frac{3.1\times10^{-17}}{I_0 g(\theta)} \frac{dT(\theta)}{dp} \text{ cm}^2, \quad (1)$$

where the constant is a conversion factor from target gas density to the measured pressure at room temperature. $T(\theta)$ is the measured beam intensity reaching the detector at scattering angle θ, I_0 is the incident beam intensity, p is the scattering gas pressure in Torr, and $g(\theta)$ is a geometric factor determined by the region of the scattering gas volume contributing to the measured signal. The value of $g(\theta)$, which is calculated from the known apparatus geometry, depends on the scattering path length and on the solid angle subtended by the detector at the scattering angle.[6] In the present experiment $\sigma(\theta)$ is determined from the slopes of the scattered beam intensity vs scattering gas pressure curves. The scattered signal is measured by a ratemeter reading the beam intensity reaching channeltron C1 (Fig. 1) with no voltage on the electrostatic analyzer. Over the energy range where cross-section results are presented, the detection efficiency of C1 is close to 100%. The incident beam intensity is generally determined by a Faraday cup. A motor-driven leak valve admits target gas to the scattering cell where the pressure is measured by a capacitance manometer. Figure 2 shows a typical data set taken at 2.0 keV and over the angular range from 2.0 to 3.0 deg. To ensure the reliability of the data each plot is made as the pressure is increased to its maximum value and then brought down to the starting low pressure. The data are discarded if the curve does not retrace properly. In addition to

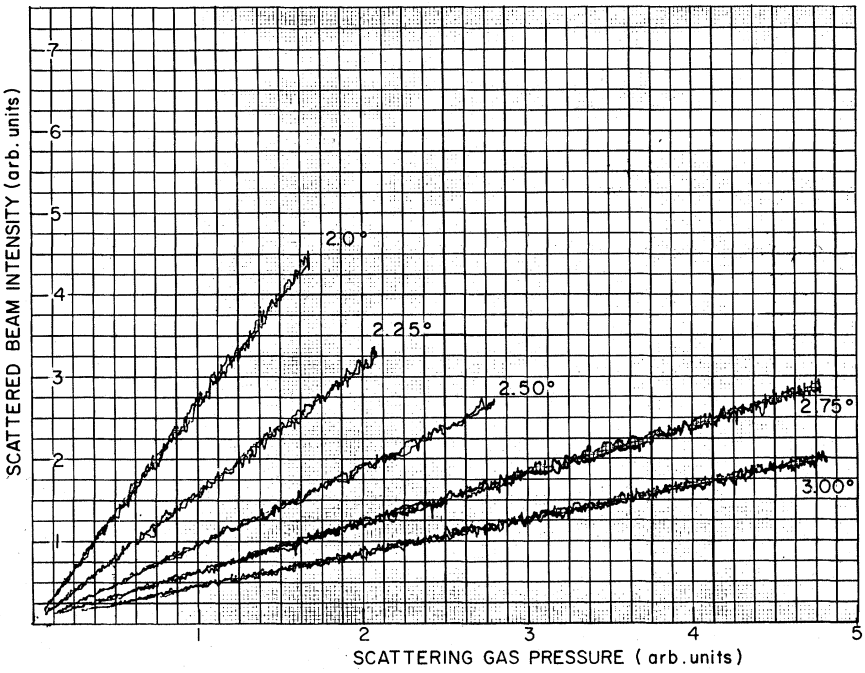

FIG. 2. Total scattered beam intensity as a function of scattering gas pressure at 2.0 keV in the angular range from 2.0 to 3.0 deg. Each plot is made by an X-Y recorder as the pressure is increased to its maximum value and then brought down to the starting low pressure. Data are discarded if the curve does not retrace properly.

providing reliable data the technique continuously demonstrates that single-collision conditions are met. Figure 3 shows the resulting differential cross sections at energies between 1.0 and 3.0 keV. Because of possible differences in detection efficiencies between the Faraday cup and channeltron C1 the cross sections are reported in arbitrary units.

B. Charge exchange

Charge-exchange scattering is studied[2] for energies between 0.5 and 3.0 keV and out to a maximum angle of 12°. $P_0(\theta)$, the probability of charge exchange is defined as

$$P_0(\theta) = N(\theta)/[N(\theta) + I(\theta)] \qquad (2)$$

and is determined from a simultaneous measurement of $I(\theta)$ (the number of ions detected at scattering angle θ) and of $N(\theta)$ (the number of neutral atoms detected at scattering angle θ). The measurements are made[7] by fully opening the slits on the electrostatic energy analyzer and applying a suitable potential to the rear analyzer plate which ensures collection of all the scattered ions by channeltron C2. The scattered neutral atoms are detected by C1, and it is demonstrated that the detection efficiency is the same for C1 and C2.[6] Figures 4 and 5 give the results of these measurements in terms of P_0 plotted as a function of τ, the reduced scattering angle (defined as $E_0\theta$, where E_0 is the incident energy). Charge-exchange processes are seen to be important and occur in a large fraction of the collisions.

The total cross section for charge exchange in $He^+ + H_2$ was measured by Stedeford and Hasted,[8] and the dominant process was assumed to be

$$He^+ + H_2 \rightarrow He^0 + H_2^+(2p\sigma_u) \rightarrow He^0 + H^+ + H(1s)$$

from arguments based on the adiabatic hypothesis. Preliminary results of a recent investigation of charge exchange (in $Ar^+ + CO$) using a time-of-flight measurement for state identification demonstrated that the adiabatic hypothesis may in fact not be applicable to ion-molecule collisions.[9] Optical analysis of $He^+ + H_2$ charge-exchange scattering[10,11] indicated that the primary source of detected radiation was due to final collision products

$$He^0 + H^+ + H(n \geq 2).$$

The conclusion of these early experiments is that charge-exchange processes, resulting in bound-state excitation of H_2^+ are weak. Optical studies generally must be interpreted with caution since they cannot respond to collisions resulting in ground-state final products. Although it is not possible to identify the specific processes from the present studies, the general shape of the curves in Figs. 4 and 5 suggests that at least two different processes are involved. The problem may be resolved in the near future by time-of-flight measurements on the scattered He^0, which could yield direct information on the states excited.

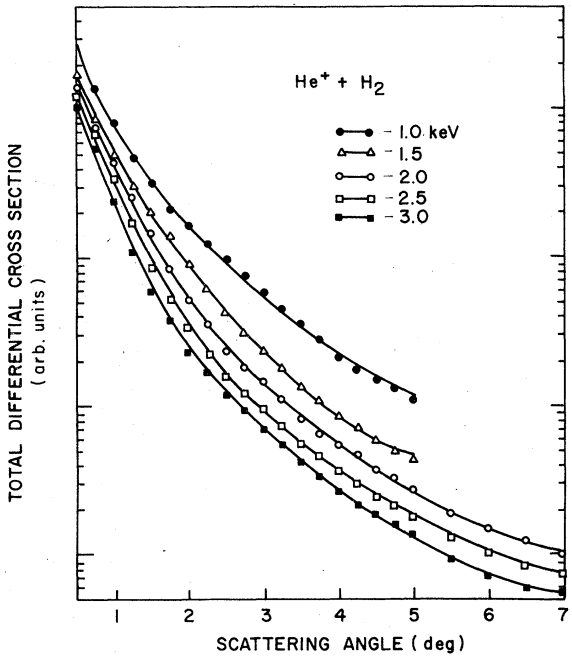

FIG. 3. Total differential cross sections for scattering in $He^+ + H_2$ collisions. The cross sections shown contain contributions from scattered He^+ and He^0 in an angular region from 0.5 to 7.0 deg.

C. Direct scattering

The energy-loss spectra of the scattered He^+ show the presence of four dominant peaks labeled A, B, C, and D. The quantity of physical interest in this experiment is Q, the inelastic energy loss which permits identification of the states excited. Energy-loss spectra obtained in collision experiments however do not directly yield Q values, which must be calculated from the data and require a knowledge of the projectile and target masses. It may be shown[1,6,12] that for elastic scattering of a projectile of mass m_1 by a target of mass m_2, the kinetic energy loss of the scattered projectile (ΔE_{el}) is given at small angle by

$$\Delta E_{el} = (m_1/m_2)E_0\theta^2 . \quad (3)$$

For inelastic scattering ΔE, the energy loss of the scattered beam is given by

$$\Delta E = \Delta E_{el} + Q \quad (4)$$

at these small angles. There are two limiting approaches to the problem of inelastic ion-molecule collisions. The binary-encounter approach assumes that inelastic scattering results from an initially elastic collision between the incident projectile and one of the atoms in the molecule. Conservation of energy and momentum applied to

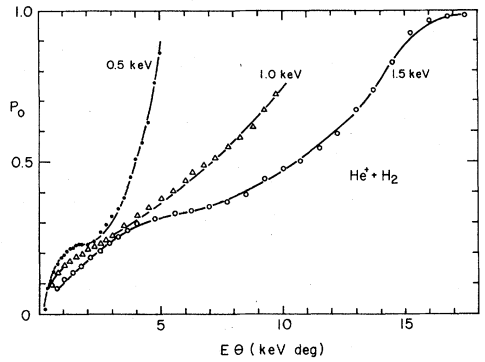

FIG. 4. Probability of charge exchange as a function of reduced scattering angle.

the recoil target molecule (after the collision) then results in molecular excitation. In the molecular-encounter approach to the problem, the entire target molecule participates in the scattering. By measuring the energy of the scattered He^+ as a function of angle and using Eq. (3), it is possible to determine the mass of the target. Figure 6 shows plots of the kinematically required [Eq. (3)] energy losses for elastic scattering in $He^+ + H$ (upper solid curve) and in $He^+ + H_2$ (lower solid curve) collisions as well as the experimentally measured energy-loss values found at the position of the maximum of peak A. It may clearly be seen that the collision is molecular (at these energies) and basically elastic out to values of $E_0\theta^2 \approx 8$ keV deg^2. For $E_0\theta^2 > 8$ keV deg^2 the energy losses indicate the presence of inelastic scattering resulting from the excitation of low-lying vibro-rotational levels of the H_2 ground electronic state. Of particular significance is that the experimental points taken at different energies are reasonably well fitted by a single curve. Peak A may then be attributed to

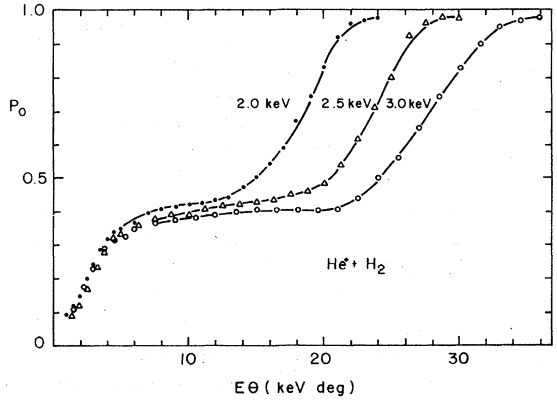

FIG. 5. Probability of charge exchange as a function of reduced scattering angle.

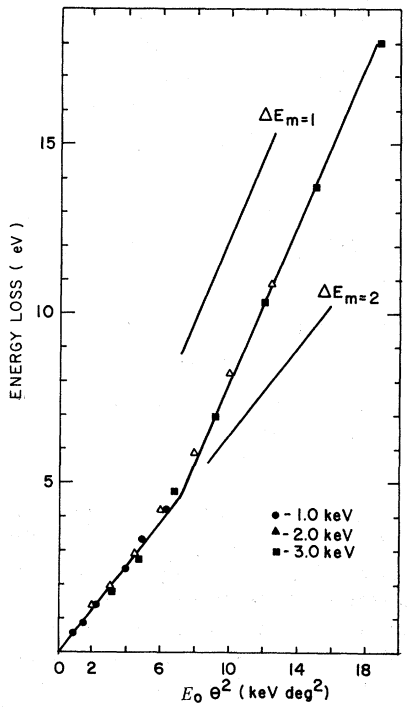

FIG. 6. Measured energy loss at the position of the maximum of peak A. The curves labeled $\Delta E_{m=1}$ and $\Delta E_{m=2}$ show the kinematically required energy losses for elastic scattering from H and H_2, respectively. The results show the collision to occur with the entire molecule and to be basically elastic out to $E_0\theta \approx 8$ keV deg^2.

a "quasielastic" scattering process.

Experimental cross-section results are conveniently presented in terms of a ρ (the reduced differential cross section) vs τ plot. At small scattering angles

$$\rho = \theta^2\sigma(\theta), \tag{5}$$

where θ and $\sigma(\theta)$ are in the laboratory frame in this paper. In ion-atom and atom-atom collision studies[12,13] this form of presentation is generally used to infer the interparticle separation at which a particular inelastic channel opens. Although this separation is not well defined for ion-molecule collisions the ρ-vs-τ plot is shown to be useful. In the present work ρ for a particular process is obtained from the measured differential cross sections taken in conjunction with the P_0 values and the relative heights of the peaks in the ELS spectra. Figure 7 shows ρ vs τ for peak A. The monotonic decrease in ρ with increasing τ is characteristic of elastic scattering at small values of the scattering angle. The curves are unnormalized in order to display the small velocity dependence of the reduced cross sections (which is not unusual even in atom-atom collisions[13]).

The inelastic peak, labeled B, exhibits several interesting features. The first is that at the energies and scattering angles investigated, the position of the maximum in the peak always appears at an energy of 13.3 eV below that found for the maximum in peak A. This strongly suggests that the vibrational and electronic excitation continue to occur independently in the collision. The vibrational excitation becomes important for $E_0\theta^2 > 8$ keV deg^2 as may be seen in Fig. 6 for peak A. The second notable feature is evident in Fig. 8 which is a plot of ρ vs τ. The experimental results (unnormalized) are seen to lie on a universal curve displaying a well-defined maximum for $\tau \approx 3.0$ keV deg. A similar behavior of the ρ-vs-τ curves is characteristic of an inelastic channel excited via a "curve-crossing" in the quasimolecule representing an ion-atom or atom-atom collision. The location of the maximum in Fig. 8 suggests that when the He^+ projectile penetrates into a critical projectile-target separation (here corresponding to $E_0\theta \approx 3$ keV deg) the inelastic channel "opens." It is not possible at this time to uniquely identify the H_2 state (or states) responsible for peak B, but any identification must be made from data taken at the smallest angles. The measured 13.3-eV loss would allow excitation of the $a\,^3\Sigma_g^+$ and the $E,F\,^1\Sigma_g^+$ states[14] into low-lying vibrational levels which are in good agreement with the Franck-Condon principle. Peak B is generally well defined, and little broadening or skewing effects are seen with increasing scattering angle.

The peaks labeled C and D represent collisions

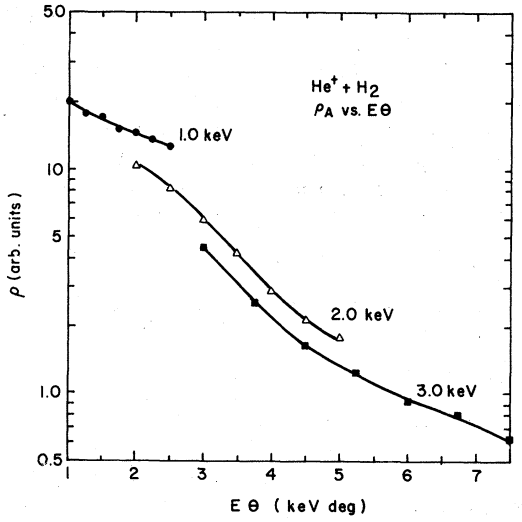

FIG. 7. Reduced cross section as a function of reduced scattering angle for peak A at τ values from 1.0 to 7.5 keV deg.

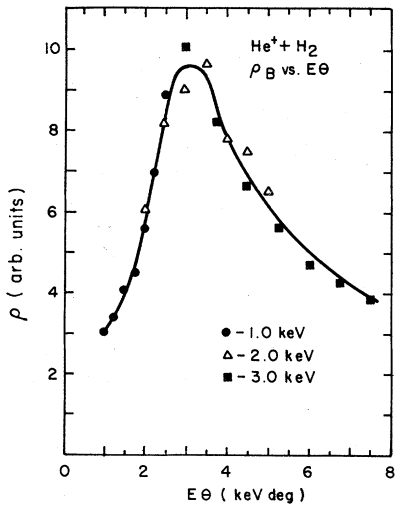

FIG. 8. Reduced cross section as a function of reduced scattering angle for peak B. The experimental points at the different energies are unnormalized. At 3 keV deg the cross section for elastic scattering is larger by a factor 5.

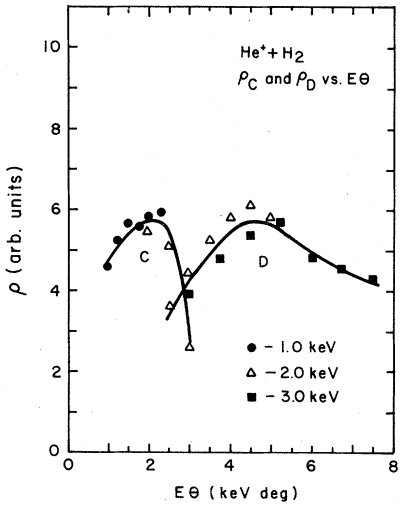

FIG. 9. Reduced cross sections as a function of reduced scattering angle for peaks C and D. The experimental points at the different energies are unnormalized, and the scale is the same as in Fig. 8.

with inelastic energy losses (measured at the positions of the maxima) of 17 and 31 eV greater respectively than that associated with peak A. The same losses are found at all energies and scattering angles where the peaks are seen. The interpretation in these cases is the same as in the case of peak B, namely the independence of the electronic and additional vibrational excitation (at the maxima) in the collision. The reduced differential cross sections as functions of reduced scattering angle are shown in Fig. 9 for peaks C and D. Universal curves are again seen to provide reasonable fits to the experimentally determined points. These curves are again unnormalized. Peak C is most likely due to the excitation of the H_2^+ $X\,^2\Sigma_g^+$ state into a vibrational level which is found to be in agreement with a Franck-Condon transition at small scattering angles. The peak is found to broaden with increasing scattering angle, suggesting dissociation[1] of the target to $H^+ + H(1s)$. For $\tau > 3$ keV deg this channel is only weakly excited. Peak C may also contain contributions from $H^+ + H^-$. Peak D represents excitation of the repulsive $2p\sigma_u$ state of H_2^+. The peak shows the broadening and skewing effects associated with the excitation followed by dissociation of the target.

The well-defined behavior of the reduced-cross-section plots for the direct inelastic scattering suggests a similar analysis on the charge-exchange scattering. This is presented in Fig. 10 for the small-angle charge exchange at 2.0 keV. The cross section is again seen to display the behavior characteristic of an inelastic process occurring at a particular projectile-target separation. The maximum in the cross section occurs for $\tau = 3$ keV deg, which is at the same location as found for peak B (Fig. 8). It should also be pointed out that the reduced differential cross sections for both peaks C and D fall off near $\tau = 3$ keV deg while the corresponding reduced cross section for charge exchange has its maximum value there. In all three processes an electron has

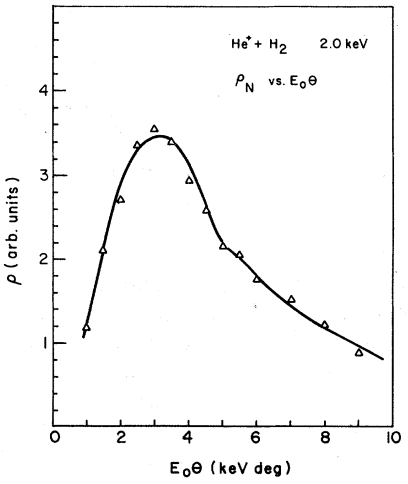

FIG. 10. Reduced cross section as a function of reduced scattering angle for the small-angle charge-exchange process.

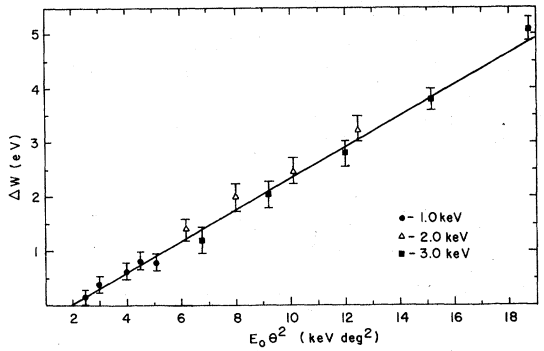

FIG. 11. Corrected FWHM for peak A. The results at all energies are seen to be fitted by a single curve.

been removed from the molecule. In both processes C and D the electron is ejected from the "system," while in the charge-exchange process it is captured into a bound He state. The results indicate that the interaction occurring at $\tau = 3$ keV deg favors the bound-state process, while those occurring for somewhat larger or smaller value of τ favor electron ejection.

An interesting feature of the vibro-rotational excitation of peak A is found from an analysis of its width as a function of scattering angle. Since the current apparatus resolution is insufficient to resolve individual vibrational levels, the width of this peak is used to indicate the extent of vibro-rotational excitation in the quasielastic scattering. In general, the measured energy width of a peak in a collision experiment depends on (1) the energy spread in the incident beam, (2) the resolution of the energy analyzer, and (3) the reduced scattering angle and angular resolution of the apparatus.[4,12] This last contributing factor is obtained from Eq. (3) and given by

$$\delta E(\theta) = 2(m_1/m_2) E_0\theta\, \delta\theta = 2(m_1/m_2)\tau\, \delta\theta, \qquad (6)$$

where $\delta\theta$ is the angular resolution. The broadening δE represented by Eq. (6) is due to kinematic and angular resolution effects. An approximate value of $\Delta W(\theta)$, the vibro-rotational broadening, may be obtained from

$$\Delta W(\theta) = W(\theta) - W_0 - \delta E(\theta), \qquad (7)$$

where $W(\theta) - W_0$ is the difference between the measured (FWHM) energy spread in the scattered and incident beams and $\delta E(\theta)$ is calculated from Eq. (6). Figure 11 shows the results of this analysis with ΔW plotted vs $E_0\theta^2$. Of particular significance is the finding that the resulting values of ΔW, at the energies studied, are reasonably well fitted by a single curve.

III. CONCLUSIONS

The present work on $He^+ + H_2$ shows that inelastic collisions involve an interaction of the He^+ with the entire molecule. In particular the observed inelastic scattering does not follow an elastic encounter with one of the atoms in the molecule as is required in a binary collision model. A similar result was obtained in studies on the $Ar^+ + N_2$ system.

Charge exchange is found to be important in $He^+ + H_2$ and at least two different processes are involved. The participating states are not identified at this time, but the problem may be resolved by a time-of-flight energy-loss measurement on the scattered He^0.

The direct scattering in $He^+ + H_2$ shows the presence of four peaks in the energy-loss spectra. The peaks represent the participation of the ground electronic and of selected electronically excited states of the molecule. The participating molecular states are initially excited via a vertical transition, on the H_2 potential energy curves,[14] which is in reasonable agreement with predictions of the Franck-Condon principle. As the scattering angle increases, the additional vibro-rotational excitation at the maxima of the peaks is found to be independent of the particular excited electronic state. Similar results were obtained in $Ar^+ + N_2$.

The energy at the maximum of peak A corresponds to elastic scattering for $E_0\theta^2 < 8$ keV deg^2. For $E_0\theta^2 > 8$ keV deg^2 vibro-rotational excitation becomes important. The width of this peak increases with increasing $E_0\theta^2$, and this width falls on a universal curve when it is plotted vs $E_0\theta^2$ at the energies studied. Since $E_0\theta^2$ is proportional to the square of the momentum transferred to the target molecule (for small scattering angles), the break away from the elastic scattering curve at $E_0\theta^2 \approx 8$ keV deg^2 indicates that there is a threshold value of momentum transfer to the molecule required for significant vibro-rotational excitation. The threshold value should depend only on the target molecule, and it would be interesting to compare results using different incident ions.

Of particular significance in $He^+ + H_2$ is that the ρ-vs-τ plots, for the observed inelastic channels, are well fitted by universal curves. This behavior of the reduced cross sections strongly suggests that the inelastic scattering proceeds via interactions occurring at fixed projectile-target separations.

Collisions spectroscopy and the analysis in terms of ρ-vs-τ plots are shown to be useful even for ion-molecule systems.

*Supported by the U.S. Army Research Office–Durham and the University of Connecticut Research Foundation.

†Present address: Planning Systems Inc., McLean, Va. 22101.

‡From part of a thesis submitted by A. V. Bray to the Graduate School at the University of Connecticut in partial fulfullment of the requirements for the Ph.D. degree.

[1]S. M. Fernandez, F. J. Eriksen, A. V. Bray, and E. Pollack, Phys. Rev. A 12, 1252 (1975).

[2]A. V. Bray, J. D. Clark, and E. Pollack, Bull. Am. Phys. Soc. 18, 1516 (1973).

[3]A. V. Bray, D. S. Newman, D. F. Drozd, and E. Pollack, in *Ninth International Conference on the Physics of Electronic and Atomic Collisions, Seattle*, 1975 (University of Washington Press, Seattle, 1975), p. 627.

[4]F. J. Eriksen, S. M. Fernandez, A. V. Bray, and E. Pollack, Phys. Rev. A 11, 1239 (1975).

[5]A. V. Bray, F. J. Eriksen, S. M. Fernandez, and E. Pollack, Rev. Sci. Instrum. 45, 429 (1974).

[6]A. V. Bray, Ph.D. thesis (University of Connecticut, Storrs, Conn., 1975) (unpublished).

[7]S. M. Fernandez, F. J. Eriksen, and E. Pollack, Phys. Rev. Lett. 27, 230 (1971).

[8]J. B. H. Stedeford and J. B. Hasted, Proc. R. Soc. Lond. A 227, 474 (1954).

[9]A. L. Goldberger, D. S. Newman, M. Vedder, and E. Pollack, Bull. Am. Phys. Soc. 22, 115 (1977).

[10]G. H. Dunn, R. Geballe, and D. Pretzer, Phys. Rev. 128, 2200 (1962).

[11]R. C. Isler and R. D. Nathan, Phys. Rev. A 6, 1036 (1972).

[12]Q. C. Kessel, E. Pollack, and W. W. Smith, in *Collisional Spectroscopy*, edited by R. G. Cooks (Plenum, New York, 1977) Chap. 2.

[13]J. C. Brenot, D. Dhuicq, J. P. Gauyacq, J. Pommier, V. Sidis, M. Barat, and E. Pollack, Phys. Rev. A 11, 1245 (1975).

[14]T. E. Sharp, At. Data 2, 119 (1971).